

THE SIMULATION OF ENERGETIC PARTICLE COLLISIONS WITH SOLIDS—A VISUAL REPRESENTATION

ROGER WEBB

Electronic and Electrical Engineering Department, University of Surrey, Guildford GU2 5XH, U.K.

ROGER SMITH

Department of Mathematical Sciences, Loughborough University of Technology, Leicestershire, LE11 3TU, U.K.

AND

ERIC DAWNKASKI, BARBARA GARRISON AND NICHOLAS WINOGRAD

Department of Chemistry, Penn State University, University Park, PA 16802, U.S.A.

SUMMARY

A set of animated sequences of various ion and cluster impacts on different material substrates is shown. The ion/target combinations used for these are: 25 keV Ar impact on Rh{100}; 500 eV B on Si{110} and C₆₀ on graphite {0001}. Molecular dynamics simulations using many body potentials are used throughout the calculations. Various aspects of both the collision process and the simulation technique are demonstrated:

- (1) the difference between individual ion impacts, in which a high sputtering event is contrasted with a low sputtering event;
- (2) the propagation of energy in a collision cascade, in which it is observed that the high energy portion of the cascade propagates outwards while the inner portion loses energy;
- (3) the number of collisions in a cascade which are non-binary in nature is shown to be significant and a number of five-body interactions are found for quite energetic interactions;
- (4) implantation from the viewpoint of the ion, in which two particles are followed, one channelling and one dechannelling. The dechannelling event leads to a focused collision sequence, which is illustrated;
- (5) the impact of a large cluster impact in which a large acoustic wave is seen to spread across the surface and evidence of a hypersonic energy transport mechanism prior to this.

1. INTRODUCTION

The purpose of this text is to describe the basis of a set of computer animated sequences of kiloelectronvolt-range particle bombardment events. We have used various ion and cluster impacts on different material substrates.

It is often a problem in the simulation of thousands of particles, all of which may be moving at once, to both explain and visualize what is happening. One method of observing the simulation results is to use computer graphics to draw the position of every particle and animate the path of each particle as the whole system evolves in time. In this way it is possible

to get an appreciation for the correlated motion of particles. For example in kiloelectronvolt-range particle bombardment it is also possible to observe when particles are ejected from the surface of the solid after the ion impact and to witness the state of the target during these processes. This text is largely descriptive and illustrative with stills from such animated sequences.

The simulation models used have been well described in the past¹⁻³ and are based on the 'molecular dynamics' codes of the late Don E. Harrison Jr, which use many-body potentials to describe the interactions among the atoms in the target matrices. For the Rh–Rh interactions, the 'embedded atom method' potential^{4,5} based on the method of Daw and Baskes is used. For the Ar–Rh interactions, the modified Moliere pair potential⁶ is used. For the B–Si interactions, the 'universal' pair potential⁷ is used. For the Si–Si interactions, the many-body potential of Tersoff⁸ is employed. Finally, for the C–C interactions in the case of fullerene and graphite, the many-body Tersoff carbon⁹ potential is used. All of these have been used extensively in the past and approach the current state-of-the-art. The crystal sizes were chosen to be as large as we could run computationally for these few individual trajectories.

2. 25 keV Ar → Rh{100}

2.1. Example 1

In the first example, the difference between choice of impact point is shown in Figure 1. In Figure 1(a), the original state of the Rh lattice containing 7688 atoms is shown. The large particle on top is the ion, just prior to its first interaction with a Rh atom. Figure 1(b) shows what happens to the surface after the initially 25 keV Ar ion has been allowed to interact with the Rh crystal. In this case, the Ar enters a crystallographic channel in the Rh crystal and passes completely through the target causing minimal disruption to the surface. Figure 1(c) shows what happens if the Ar ion's initial impact point is moved so that now, instead of passing right through the Rh crystal, it has a hard collision with a third layer Rh atom which causes the Rh atom and the Ar ion to recoil in opposite directions, passing laterally below the surface, in turn causing much displacement and particle ejection from the surface. In general, a complete set of different impact points is made up of these 'low' and 'high activity' events.¹⁰ The probabilities of each type of event depends upon the ion/target combination, the crystal structure and the bombardment conditions – ion energy, angles of incidence, etc

2.2. Example 2

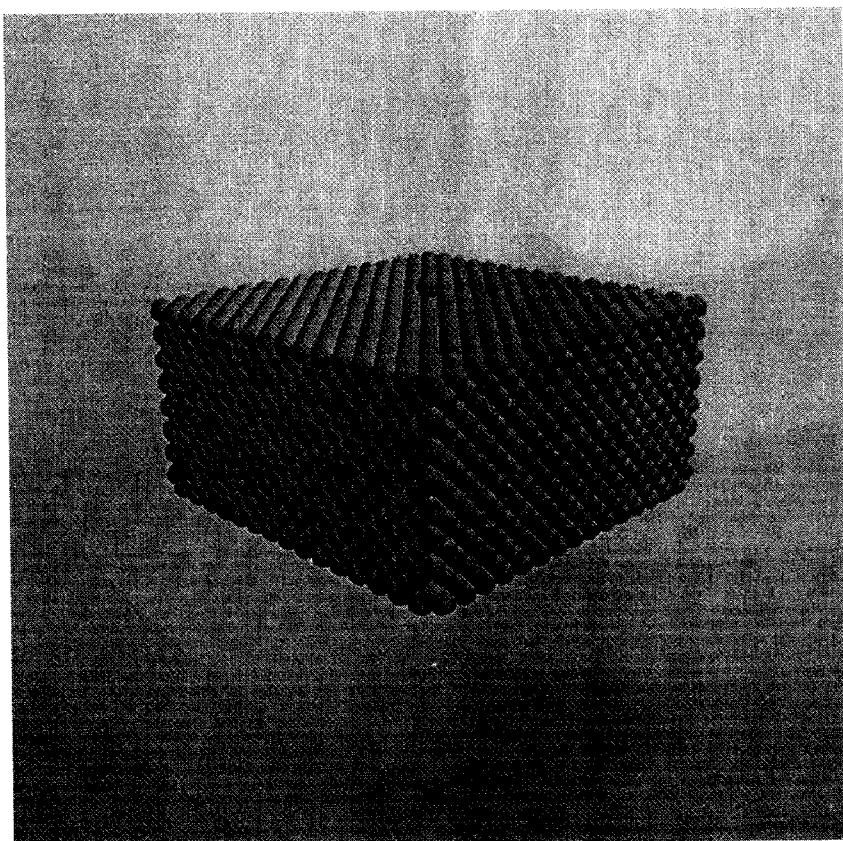
In the second example the high surface activity trajectory is used to show the way in which energy is propagated through the crystal by the ensuing collision cascade. The atoms of the crystal are drawn smaller and the crystal rotated to align the crystal planes so that it is possible to see more easily into the crystal. The Rh atoms are then drawn larger once they have sufficient energy to start moving and are coloured – in the animated sequences – depending on their total energy, i.e. the sum of their kinetic and potential energies. It is quite easy to see, from the animated sequence that energy propagates outward from the initial cascade region via a number of mechanisms. Fast recoils can be seen leaving the region and a large number of replacement collision sequences transport energy quickly long distances, while the transport of particles is only to their nearest neighbour sites.

2.3. Final sequence

The final sequence using the Ar–Rh combination is an investigation of multiple collisions. In all our molecular dynamics simulations, we directly integrate Newton's laws of motion, thus virtually all atoms simultaneously interact with all other atoms, unless of course they have been sputtered into the gas phase. However, many other workers use the binary collision approximation.¹¹ It is illustrative, therefore, to try to determine the number of binary collisions versus multiple collisions. We thus use the high activity trajectory to illustrate many-body collisions. The first problem to overcome is that in molecular dynamics it is difficult to define a *collision* because, since all particles are always interacting with each other, all particles are forever in 'contact' or 'collision' with each other. But not all of these interactions are significant enough to cause displacement motion. Consequently, we define a parameter:

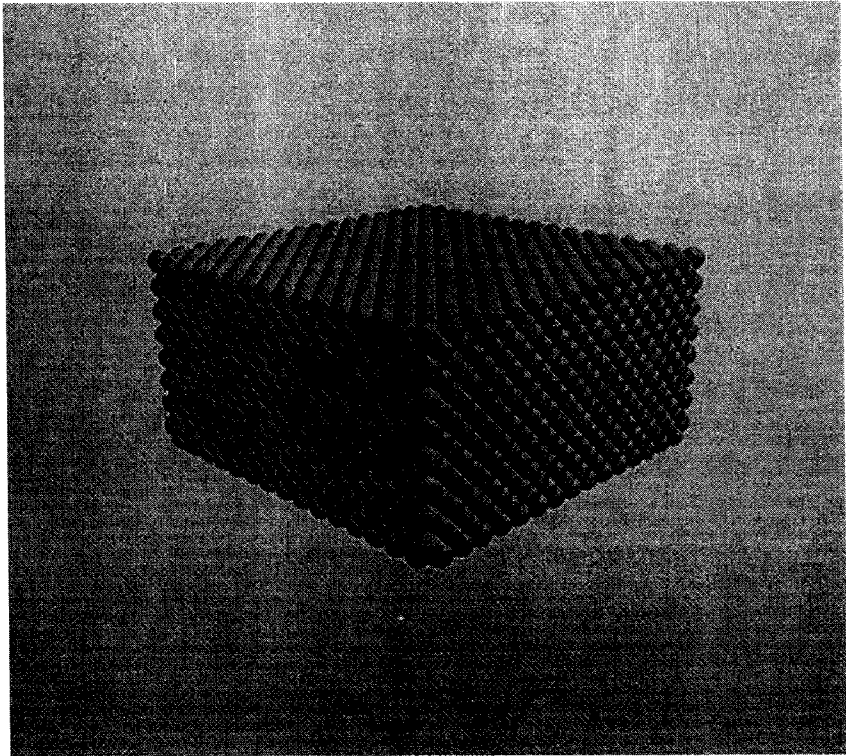
$$FF = \sum_j |F_{ij}|$$

where F_{ij} is the force on particle i from particle j . If $FF > 3 \times 10^{-13}$ newtons, then the particle

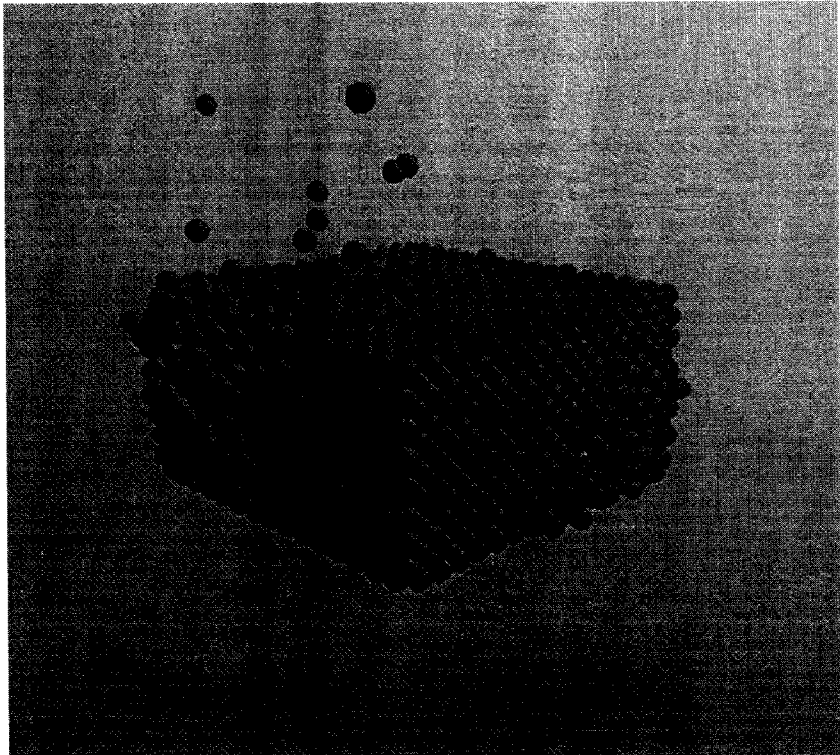


(a)

Figure 1. This figure illustrates the first two sequences of the video. It shows the different ways in which a surface reacts to the same ion bombardment by changing only the initial impact point. The high surface activity event is then used in further sequences to illustrate the quenching of the energetic-particle-generated cascade of target atoms and the number of multiple collisions: (a) rhodium crystal at start of calculation, 25 keV argon ion poised above surface; (b) state of rhodium crystal after argon ion is released at an impact point and direction which causes significant channelling of the ion; (c) state of the rhodium crystal after the argon ion is released at an impact point such that the ion undergoes substantial energy loss close to the surface



(b)



(c)

Figure 1. *Continued*

is considered to have undergone a collision. The value must be high enough to emulate the displacement energy used in binary collisions models. The value used has been varied and higher values result in particles moving without having had a collision. The value used appears to capture most of the moving particles. We use the sum of the absolute value of forces to determine FF so that in the situation where a particle passes between two (or more) particles – and hence experiences a net force of near zero – it will still be considered to have had a collision. Now, that we have defined a collision we can make some judgements upon what is a two-body, a three-body, a four-body or more collision. If only one particle contributes more than 10% to FF, then it is defined as a two-body collision, if two particles contribute more than 10% each to FF, then the collision is a three-body one; if three particles contribute more than 10% each to FF, then the collision is a four-body one; if four (or more) particles contribute 10% each to FF then the collision is a five(ish)-body one.

Using these definitions of collisions, the atoms are then coloured depending upon the number of ‘bodies’ involved in the collision – if the particle is not colliding, it is drawn small and green; two-body collisions are drawn large and green. Other multiple-body collisions are drawn large and coloured. It is clear from the animated sequence that a substantial number of three- and four-body collisions occur during the cascade, and it is possible to see a few five-body collisions. The higher-order collisions occur mostly during the peak activity of the cascade shown in Figure 2, which plots the number of many-body collisions against interaction time. It can be seen that the fraction of two-body collisions decreases in favour of the higher-order collisions when the total number of collisions is at its maximum. As the cascade proceeds, the number of collisions decreases as the energy of the particles decreases; because of this, the number of many-body collisions decreases. It should be remembered, however, that this means that as the number of many-body interactions increases, these will dominate. Also, the cascade expands beyond the size of the crystal dimensions after 150–200 fs and thus the behaviour after this time is less believable.

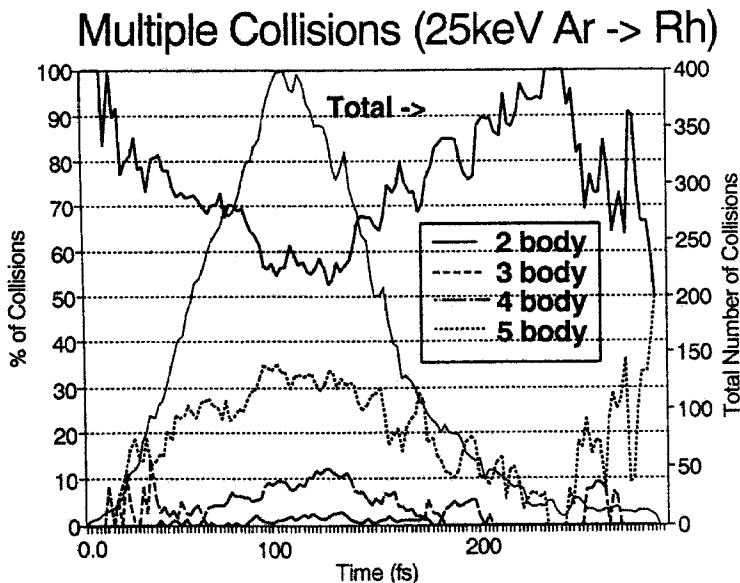


Figure 2. Distribution of multiple collisions as a function of the lifetime of the high activity cascade. A significant number of multiple (more than binary) collisions is observed during the peak activity of the cascade

3. 500 eV B \rightarrow Si{110}

This set of sequences shows implantation from the point of view of the ion.

3.1. *First sequence*

In the first sequence, we experience the helical path of a channelling B ion as it passes along a single crystal silicon axial channel as shown in Figure 3. We use perspective and directional lighting to enhance the image and to give the impression of channelling from the ion's viewpoint. The silicon atoms are shaded green and a single {100} channel is picked out with blue atoms to show how well the boron is channelled. The viewing direction is the same as the direction of motion of the particle. Because the particle is channelling, one of the components of the velocity dominates over the other two. However, from time to time the particle undergoes small-angle collisions that, while causing only little changes in the main component of the velocity, can make large relative changes in the minor components, thus making the particle viewing direction rotate about the primary viewing direction.

3.2. *Second sequence*

The second of these sequences follows an ion which de-channels. Two particles are marked in blue to give a reference point in the crystal. The silicon atoms otherwise are shaded green

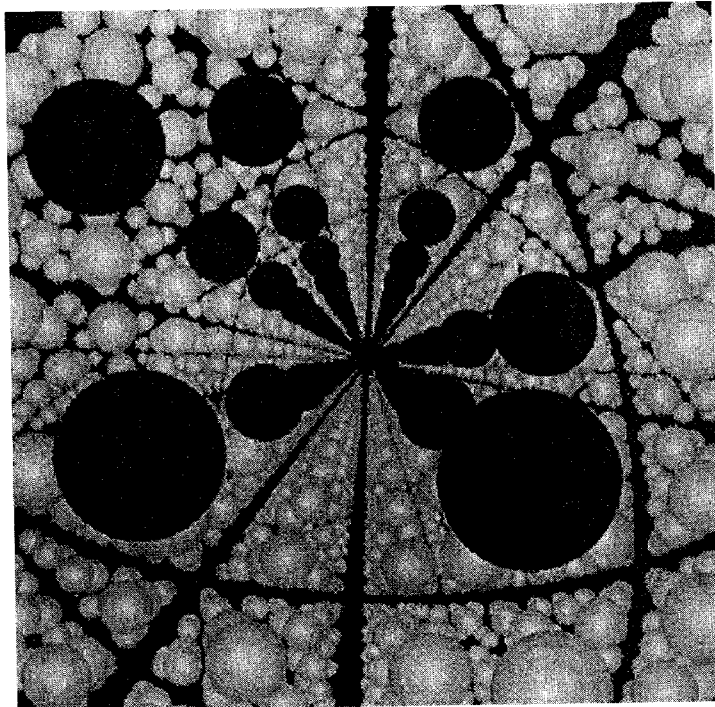


Figure 3. This next set of animated sequences from the movie demonstrates the ion penetration phenomenon. There are three sequences: a well-channelled example; a de-channelled example looking forward; and the same de-channelled example looking backward. An ion's 'eye' view of a silicon 110 channel during a well-channelled trajectory. The channel borders are marked out in a different colour

through red (50 eV) depending upon their total energy. The boron particle has a collision with a surface silicon atom – which is ultimately sputtered – and then passes close to two other atoms in subsequent layers. These collisions become apparent by short rotational activity. But the boron continues in a straight line path until it encounters the next atom, which becomes red as it picks up energy from the collision. The boron then undergoes a back-scattering event and the viewing direction changes discontinuously and is now pointing back toward the surface. The boron has lost a large fraction of its initial energy in that collision and now just drifts below the surface.

3.3. Further sequence

In a further sequence, we follow the same trajectory as above but look in the reverse direction, i.e. along the path of the boron. In this case we see the surface atom which was

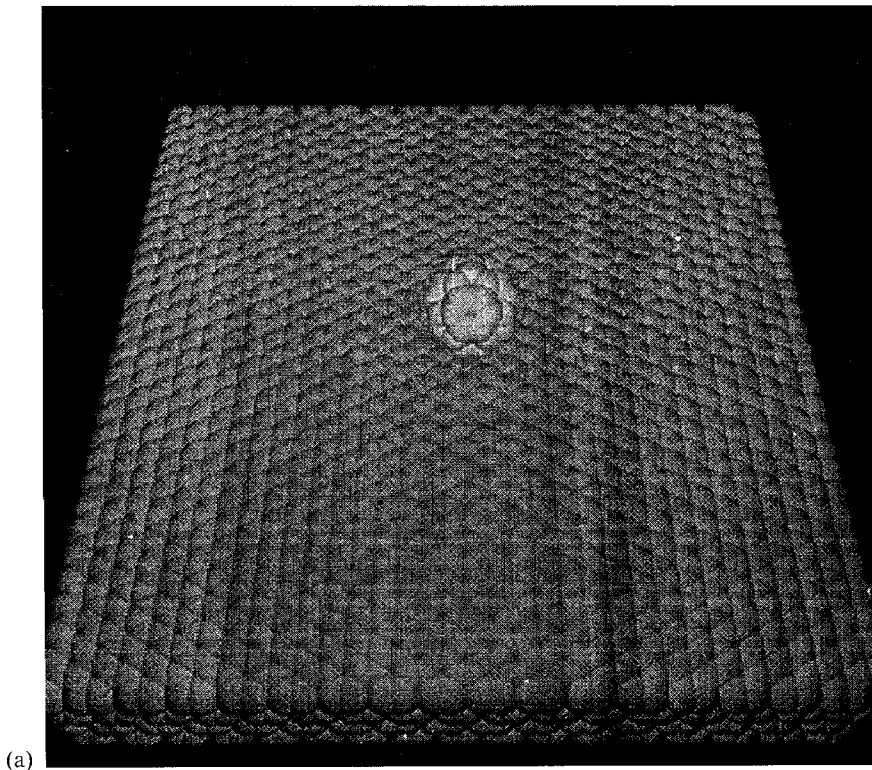
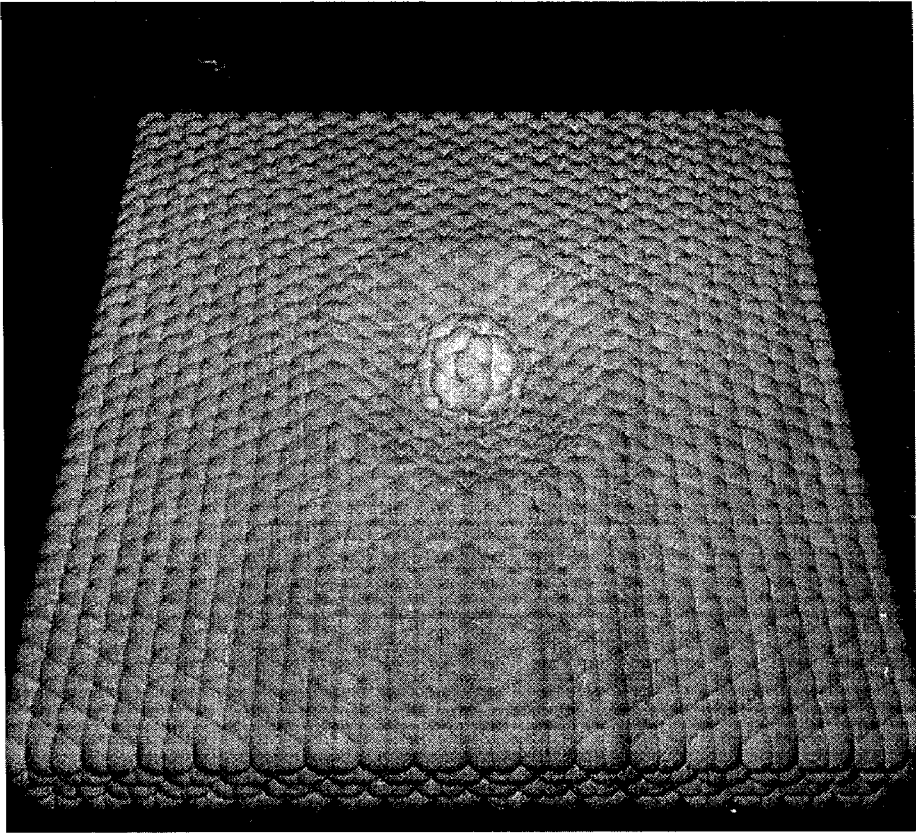
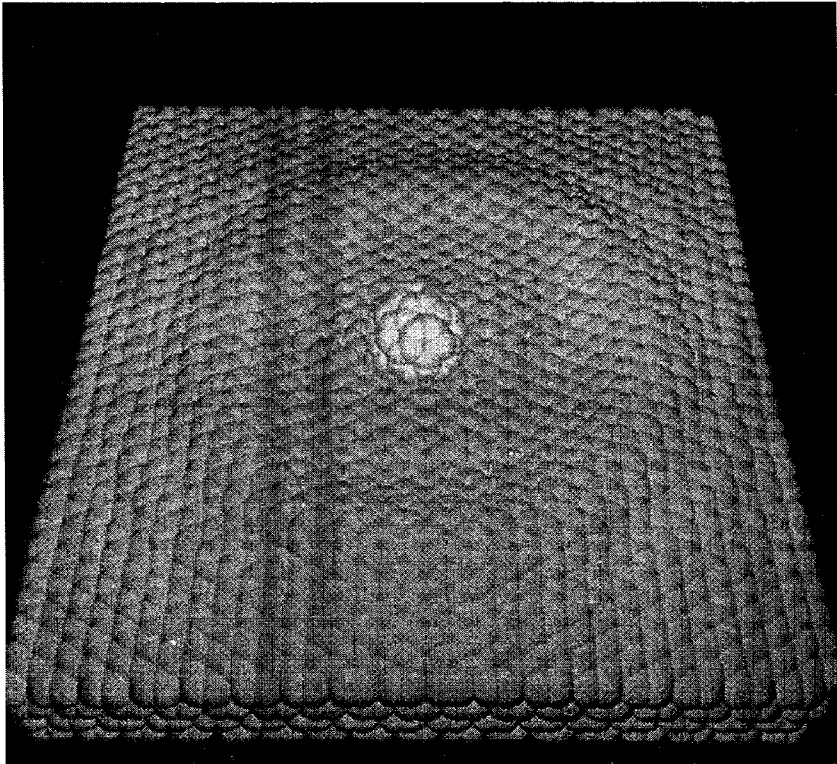


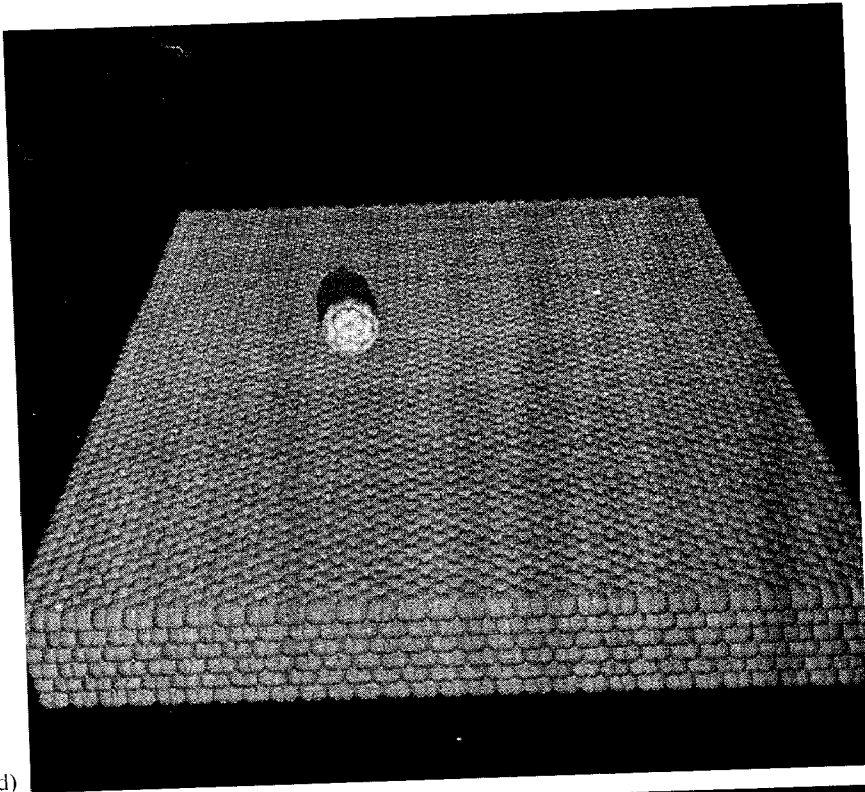
Figure 4. There are two animated sequences in the final section of the movie. The first shows the effects of a 6 keV fullerene impact on a graphite surface in which the fullerene shatters and produces an acoustic wave. The second shows a lower energy (250 eV) impact in which the fullerene remains intact and produces a similar acoustic wave. A faster – supersonic – transverse wave can also be seen propagating across the surface in advance of this acoustic wave: (a) graphite surface prior to impact of fullerene molecule; (b) graphite surface 250 fs after impact of a 250 eV fullerene molecule. An acoustic wave is seen spreading from the point of impact and the molecule compresses; (c) graphite surface 520 fs after impact of a 250 eV fullerene molecule. The acoustic wave spreads further across the surface. The molecule remains intact and adheres to the surface; (d) graphite surface prior to impact of a 15 keV fullerene molecule directed at 60 degrees to the surface; (e) graphite surface 520 fs after impact of a 15 keV fullerene molecule directed at 60 degrees to the surface. The molecule breaks up. An acoustic wave propagates away from the impact site and faster energy propagation is observed in the principle crystallographic directions



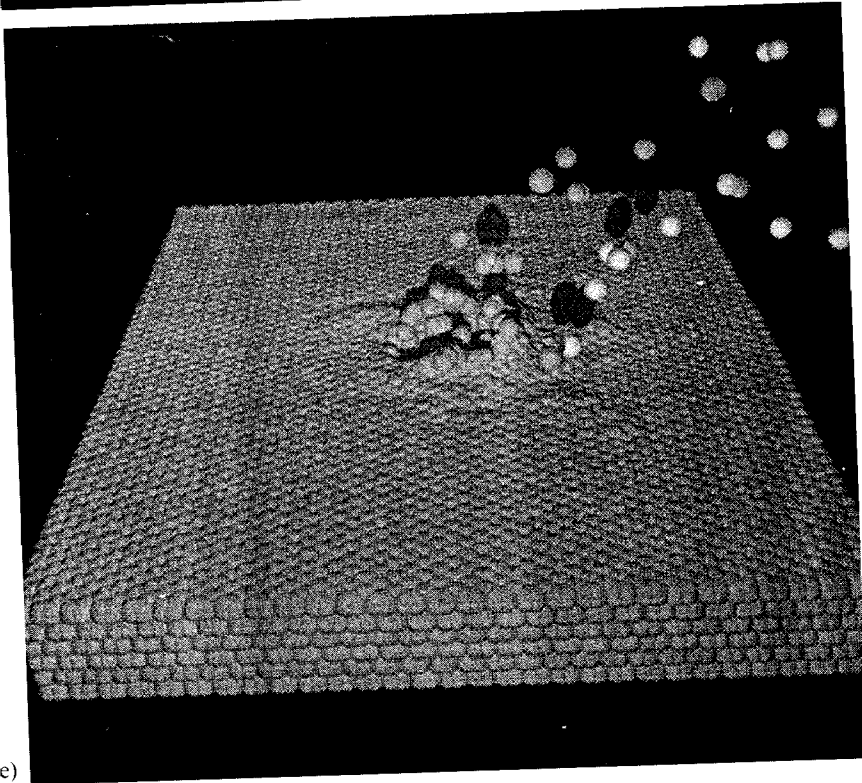
(b)



(c)



(d)



(e)

Figure 4. *Continued*

struck on entering the silicon still with enough energy for it to be coloured red – it is ultimately sputtered. The boron passes the two marked blue atoms. At this point the boron has its hard collision and suddenly the viewing direction changes and we can see the other particle involved in the back scattering collision. This energetic recoil then initiates a linear displacement sequence that propagates some distance before we stop the calculation.

4. $C_{60} \rightarrow$ Graphite{0001}

This set of sequences shows an effect of cluster bombardment on surfaces. A complete paper on this particular set of simulations is in preparation.¹² But, briefly, we have chosen a C_{60} molecule in the fullerene arrangement and directed it at a graphite surface. In this case impact point variations are much more subtle. At low energies, the fullerene strikes the surface and remains intact causing a large acoustic wave to spread out from the point of impact. Figure 4 shows the graphite surface at three different times for interactions with a molecule of initial energy 250 eV. At higher energies, the fullerene breaks up and causes some surface damage, the acoustic wave is still observed. This is seen in Figure 4. In this case, the impact occurs at 60 degrees incidence and there is evidence of preferential energy spreading in the main crystallographic directions. Initially, however, a longitudinal wave, spreading at much higher velocity and transporting only very small amounts of energy can be detected. This can be seen as a very subtle *colour* change, due to minor fluctuations in height above the surface and hence reflectivity changes. This effect is only noticeable in the movie and is the result of small displacements of the order of a tenth of an angstrom.

5. CONCLUSIONS

In conclusion, it has been shown that computer animated graphics can aid extensively in the interpretation of computer generated data. In particular, easy observation is possible of correlated motion in a system containing large numbers of interacting particles.

REFERENCES

1. D. E. Harrison Jr, P. W. Kelly, B. J. Garrison and N. Winograd, *Surf Sci.*, **B76**, 311 (1978)
2. R. Smith and D. E. Harrison Jr, *Computers in Physics*, **3**(5), 68 (1989).
3. D. E. Harrison Jr., *Crit. Rev. Solid State and Mater. Sci.*, **14**(1), S1 (1988).
4. M. S. Daw and M. I. Baskes, *Phys. Rev. Lett.*, **50**, 1285 (1983).
5. M. S. Daw and M. I. Baskes, *Phys. Rev. B.*, **35**, 7423 (1985).
6. G. Moliere, *Z. Naturforsch.*, **A2**, 133, (1947).
7. J. F. Ziegler, J. P. Biersack and U. Litmark, *The Stopping and Range of Ions in Solids*, Pergamon, New York, 1985.
8. J. Tersoff, *Phys. Rev. B.*, **38**, 9902 (1986).
9. J. Tersoff, *Phys. Rev. Lett.*, **61**, 2879 (1988).
10. D. E. Harrison Jr and R. P. Webb, *Nucl. Instrum. Meths*, **218**, 727, (1983).
11. M. T. Robinson and I. M. Torrens, *Phys. Rev.*, **B9**, 5008 (1974).
12. R. Smith and R. P. Webb, *Proc. Royal Society London A*, **441**, 495 (1993).